Networks and Heterogeneous Media

http://www.aimspress.com/journal/nhm

NHM, 18(3): 1006–1023.
DOI: 10.3934/nhm.2023044
Received: 30 December 2022
Revised: 05 March 2023
Accepted: 16 March 2023
Published: 22 March 2023

Research article

A robust adaptive grid method for first-order nonlinear singularly perturbed Fredholm integro-differential equations

Zhi Mao[1,2,*] **and Dan Luo**[2]

[1] School of Data Science, Tongren University, Tongren 554300, China
[2] School of Mathematics and Statistics, Jishou University, Xiangxi 416100, China

* **Correspondence:** Email: yjsymz@gztrc.edu.cn; Tel: +86-08568121276; Fax: +86-08568121809.

Abstract: In this paper, a robust adaptive grid method is developed for solving first-order nonlinear singularly perturbed Fredholm integro-differential equations (SPFIDEs). Firstly such SPFIDEs are discretized by the backward Euler formula for differential part and the composite numerical quadrature rule for integral part. Then both a prior and an a posterior error analysis in the maximum norm are derived. Based on the prior error bound and the mesh equidistribution principle, it is proved that there exists a mesh gives optimal first-order convergence which is robust with respect to the perturbation parameter. Finally, the posterior error bound is used to choose a suitable monitor function and design a corresponding adaptive grid generation algorithm. Numerical results are given to illustrate our theoretical result.

Keywords: Fredholm integro-differential equation; singularly perturbed problem; adaptive grid algorithm; ε-uniform convergence

1. Introduction

Consider the following singularly perturbed Fredholm integro-differential equation (SPFIDE) in the interval $\bar{I} = [0, T]$:

$$\begin{cases} Lu(t) := \varepsilon u'(t) + f(t, u(t)) + \lambda \int_0^T K(t, s, u(s))\, ds = 0, \ t \in I = (0, T], \\ u(0) = A, \end{cases} \tag{1.1}$$

where $0 < \varepsilon \ll 1$ is a perturbation parameter, A is a given constant and λ is a real parameter. We assume that $f(t, u) \in C^1\left(\bar{I} \times R\right)$, $K(t, s, u) \in C^1\left(\bar{I} \times \bar{I} \times R\right)$ and there exist constants α, β such that $0 < \alpha \le |\partial f/\partial u|$, $|\partial K/\partial u| \le \beta$. Under these assumptions, the problem (1.1) has a unique solution (see [1]).

It is well known that the SPFIDEs arise widely in scientific fields such as mathematical biology [2], material mechanics [3], hydrodynamic [4] and so on.These problems depend on such a small positive parameter ε that the solution varies rapidly when $\varepsilon \to 0$. Due to the presence of this perturbation parameter ε, classical numerical methods on a uniform mesh fail to give accurate results. Therefore, it is necessary to develop suitable numerical methods that are ε-uniformly convergent for solving these problems.

Over the past few years, there has been a growing interest in the numerical methods for Volterra integro-differential equations (see,e.g., [5–10]) and Fredholm integro-differential equations (see,e.g., [11, 12]). When the differential term of these integro-differential equations contains a small positive perturbation parameter ε, these problems are called singularly perturbed integro-differential equations. Recently, some robust numerical methods are proposed to solve singularly perturbed Volterra integro-differential equations [13–16]. Meanwhile, the authors in [17, 18] developed fitted finite difference schemes on a uniform mesh for second-order SPFIDEs and gave some convergence results based on the prior information of the exact solution. Durmaz, et.al., [19] proposed a second-order uniformly convergent finite difference scheme on a Shishkin mesh for a singularly perturbed Fredholm integro-differential equation with the reduced second type Fredholm equation. In [20], the authors presented a fitted finite difference approach on a Shishkin mesh for a first-order singularly perturbed Fredholm integro-differential initial value problem with integral condition. Kumar et al. [21] proposed a non-standard finite difference scheme with Haar wavelet basis functions for a singularly perturbed partial integro-differential equation. Recently, Cakir et al., [22] solved first-order nonlinear SPFIDEs on a Sinshkin mesh with first-order convergence rate.

From the literatures we have mentioned above, the existing numerical methods of SPFIDEs given in [19–21] are layer-adapted mesh approaches, which require a priori information about the location and width of the boundary layer. Thus, adaptive grid methods by equidistributing monitor functions are widely used to solve some singularly perturbed problems, see [25–29] for example. The advantages of these adaptive grid methods is to cluster automatically the grid points within the boundary layer. To the best of our knowledge, there is no report about this adaptive grid method for problem (1.1). Therefore, the aim of this paper is to solve problem (1.1) numerically by a finite difference scheme on an adaptive grid obtained by equidistributing a positive monitor function. The discrete scheme is constructed by using the backward Euler formula and right rectangle formula to approximate derivative term and nonlinear integral term, respectively. It is proved under some additional conditions that the proposed adaptive grid method is first-order uniformly convergent, with respect to ε.

The rest of this paper is as follows. In Section 2, preliminary results of the exact solution are laid out. A discretization scheme is established in Section 3, in which a prior error analysis and a posterior error estimate are carried out successively. Numerical results obtained by the adaptive gird algorithm are given in Section 4 to support the theoretical analyses. The paper ends with a summary of the main conclusions in Section 5.

Notation Throughout this paper, C which is not necessarily the same at each occurrence, indicates a positive constant independent of the mesh division parameter N or the singular perturbation parameter ε. To simplify the notation, we set $v_k = v(t_k)$ for any function $v(t)$. In our estimates, the maximum norm of a continuous function $v(t)$ with the domain $[0, T]$ is defined as $\|v(t)\|_\infty = \operatorname{ess\,sup}_{t\in[0,T]} |v(t)|$ as well as the maximum norm of a discrete vector $\boldsymbol{x} = \{x_i\}_{i=0}^N$ with $N+1$ elements is defined as $\|\boldsymbol{x}\|_\infty = \max_{i=0,1,2,\cdots,N} |x_i|$.

2. Preliminary results

In this section, we list the bounds for the exact solution $u(t)$ and its first-order derivative.

Lemma 2.1. *[22, Lemma 1] Assume the constant λ satisfies*

$$|\lambda| < \frac{\alpha}{\max\limits_{0\le t\le T}\int_0^T |G(t,s)|\,ds}. \tag{2.1}$$

Then we have

$$\|u\|_\infty \le C_0, \tag{2.2}$$

$$|u'(t)| \le C\left(1+\frac{1}{\varepsilon}e^{-\frac{\alpha t}{\varepsilon}}\right),\ 0\le t\le T, \tag{2.3}$$

where

$$C_0 = \frac{|A|+\frac{1}{\alpha}\|q\|_\infty}{1-\frac{1}{\alpha}|\lambda|\max\limits_{0\le t\le T}\int_0^T |G(t,s)|\,ds},$$

$$G(t,s) = \frac{\partial}{\partial u}K(t,s,\gamma u),\ 0<\gamma<1,$$

$$q(t) = -f(t,0) - \gamma\int_0^T K(t,s,0)\,ds.$$

Corollary 2.1. *For any two functions $v(t)$ and $w(t)$ satisfying*

$$v(0) = w(0) = A, \tag{2.4}$$

and

$$Lv(t) - Lw(t) = \tilde{F}(t),\ t\in I, \tag{2.5}$$

where $\tilde{F}(t)$ is a bounded piece-wise continuous function, we have

$$\|v(t)-w(t)\|_\infty \le C\,\|Lv(t)-Lw(t)\|_\infty. \tag{2.6}$$

Proof. The proof is similar to [15, Corollary 2.1]. □

3. Discretization and error analysis

3.1. Discrete scheme

Let $\bar{\Omega}_N := \{0 = t_0 < t_1 < \cdots < t_N = T\}$ be an arbitrary non-uniform mesh and $h_i = t_i - t_{i-1}$ be the local mesh size for $i = 1, 2, \cdots, N$. For a given mesh function $\{v_i\}_{i=0}^N$, define the backward finite difference operator as follows:

$$D^- v_i = \frac{v_i - v_{i-1}}{h_i},\ i = 1, 2, \cdots, N. \tag{3.1}$$

Then to construct the discretization scheme for problem (1.1), we integrate Eq (1.1) over (t_{i-1}, t_i) and use the right rectangle rule to approximate the integral part, which yield,

$$\begin{cases} \varepsilon D^- u_i + f(t_i, u_i) + \lambda \sum_{j=1}^{N} h_j K\left(t_i, t_j, u_j\right) + R_i = 0,\ i = 1, 2, \cdots, N, \\ u_0 = A, \end{cases} \tag{3.2}$$

where

$$R_i := R_i^{(1)} + R_i^{(2)} + R_i^{(3)} \tag{3.3}$$

and

$$\begin{aligned} R_i^{(1)} &= -h_i^{-1} \int_{t_{i-1}}^{t_i} (t - t_{i-1}) \frac{d}{dt} f(t, u(t))\, dt, \\ R_i^{(2)} &= -\lambda h_i^{-1} \int_{t_{i-1}}^{t_i} (t - t_{i-1}) \int_0^T \frac{\partial}{\partial t} K(t, s, u(s))\, ds dt, \\ R_i^{(3)} &= -\lambda \sum_{j=1}^{N} \int_{t_{j-1}}^{t_j} \left(s - t_{j-1}\right) \frac{d}{ds} K(t_i, s, u(s))\, ds. \end{aligned}$$

Neglecting the truncation error R_i in Eq (3.2), we obtain the discretization scheme of problem (1.1)

$$\begin{cases} L^N u_i^N := \varepsilon D^- u_i^N + f\left(t_i, u_i^N\right) + \lambda \sum_{j=1}^{N} h_j K\left(t_i, t_j, u_j^N\right) = 0,\ i = 1, 2, \cdots, N, \\ u_0 = A, \end{cases} \tag{3.4}$$

where u_i^N is the approximation of $u(t)$ at point $t = t_i$.

3.2. A prior error analysis

Let $e_i^N := u_i^N - u_i$, $i = 0, 1, \cdots, N$, be the absolute error at t_i of the numerical solution. Then we can obtain the following error equations

$$\begin{cases} L^N u_i^N - L^N u_i = R_i,\ i = 1, 2, \cdots, N, \\ e_0^N = 0, \end{cases} \tag{3.5}$$

where R_i is the local truncation error defined in Eq (3.3) at t_i.

Lemma 3.1. *For $i = 1, 2, \cdots, N$, the truncation error R_i defined in Eq (3.3) satisfies*

$$|R_i| \le C \max_{1 \le i \le N} \int_{t_{i-1}}^{t_i} (1 + |u'(t)|)\, dt. \tag{3.6}$$

Proof. At first, based on the conditions $f(t, u) \in C^1(\bar{I} \times R)$ and $0 < \alpha \le |\partial f / \partial u|$, we obtain

$$\begin{aligned} \left|R_i^{(1)}\right| &\le h_i^{-1} \int_{t_{i-1}}^{t_i} h_i \left(\left| \frac{\partial f(t, u)}{\partial t} \right| + \left| \frac{\partial f(t, u)}{\partial u} \right| |u'(t)| \right) dt \\ &\le C \int_{t_{i-1}}^{t_i} (1 + |u'(t)|)\, dt. \end{aligned} \tag{3.7}$$

Then, since $K(t,s,u) \in C^1\left(\bar{I}\times\bar{I}\times R\right)$ and $|\partial K/\partial u| \le \beta$, we have

$$\begin{aligned}\left|R_i^{(2)}\right| &\le |\lambda| \int_{t_{i-1}}^{t_i}\int_0^T \left|\frac{\partial}{\partial t}K(t,s,u(s))\right| dsdt \\ &\le Ch_i.\end{aligned} \tag{3.8}$$

and

$$\begin{aligned}\left|R_i^{(3)}\right| &\le |\lambda| \sum_{j=1}^{N} T \int_{t_{j-1}}^{t_j} \left(\left|\frac{\partial K(t_i,s,u)}{\partial s}\right| + \left|\frac{\partial K(t_i,s,u)}{\partial u}\right| |u'(s)|\right) ds \\ &\le C \max_{1\le j\le N} \int_{t_{j-1}}^{t_j} (1+|u'(t)|)\, dt.\end{aligned} \tag{3.9}$$

Finally, the desired result of this lemma can be followed by Eqs (3.7), (3.8) and (3.9). □

Lemma 3.2. *Under the assumption*

$$|\lambda| < \frac{1}{\alpha} \max_{1\le i\le N} \sum_{j=1}^{N} h_j \left|G_{ij}\right|, \tag{3.10}$$

we have

$$\left\|\boldsymbol{e}^N\right\|_\infty \le \frac{1}{\alpha}\left(1 - \frac{1}{\alpha}|\lambda| \max_{1\le i\le N} \sum_{j=1}^{N} h_i \left|G_{ij}\right|\right)^{-1} \|\boldsymbol{R}\|_\infty, \tag{3.11}$$

where $\boldsymbol{e}^N = \left\{e_i^N\right\}_{i=0}^N$, $\boldsymbol{R} = \{R_i\}_{i=0}^N$ *and* $G_{ij} = \frac{\partial}{\partial u}K\left(t_i, s_j, u_j + \zeta e_j^N\right)$, $0 < \zeta < 1$.

Proof. Applying the mean value theorem to Eq (3.5), we get

$$\varepsilon D^- e_i^N + a_i e_i^N + \lambda \sum_{j=1}^{N} h_j G_{ij} e_j^N = R_i,\ i = 1, 2, \cdots, N, \tag{3.12}$$

where

$$a_i = \frac{\partial}{\partial u} f\left(t_i, u_i + \xi e_i^N\right),\ 0 < \xi < 1, \tag{3.13}$$

$$G_{ij} = \frac{\partial}{\partial u} K\left(t_i, s_j, u_j + \zeta e_j^N\right),\ 0 < \zeta < 1. \tag{3.14}$$

According to maximum principle for the operator $\varepsilon D^- e_i^N + a_i e_i^N$, we have

$$\left\|\boldsymbol{e}^N\right\|_\infty \le \frac{1}{\alpha}\|\boldsymbol{R}\|_\infty + \frac{1}{\alpha}|\lambda| \left\|\boldsymbol{e}^N\right\|_\infty \max_{1\le i\le N} \sum_{j=1}^{N} h_j \left|G_{ij}\right|, \tag{3.15}$$

which immediately leads to the desired result with the assumption (3.10). □

Based on the above Lemmas 3.1–3.2, we get the following convergence results.

Theorem 3.1. *Let $u(t)$ be the solution of problem (1.1) and u_i^N be the solution of discrete scheme (3.4). Then*

$$\max_{1\le i\le N}\left|u_i^N-u_i\right|\le C\max_{1\le i\le N}\int_{t_{i-1}}^{t_i}\left(1+\left|u'(t)\right|\right)dt. \tag{3.16}$$

Corollary 3.1. *Under the conditions of Theorem 3.1, there exists an adaptive grid $\{t_i\}_{i=0}^N$ such that*

$$\max_{1\le i\le N}\left|u_i^N-u_i\right|\le CN^{-1}. \tag{3.17}$$

Proof. Based on the mesh equidistribution principle presented in [29], the mesh $\{t_i\}_{i=0}^N$ given by our adaptive grid algorithm satisfies

$$\int_{t_{i-1}}^{t_i}M(t)\,dt=\frac{1}{N}\int_0^T M(t)\,dt,\ i=1,2,\cdots,N, \tag{3.18}$$

where $M(t)$ is called the monitor function, which can be chosen as

$$M(t)=1+\left|u'(t)\right|. \tag{3.19}$$

Therefore, it follows from Lemma 2.1 that

$$\begin{aligned}\max_{1\le i\le N}\left|u_i^N-u_i\right|&\le C\max_{1\le i\le N}\int_{t_{i-1}}^{t_i}\left(1+\left|u'(t)\right|\right)dt\\&=\frac{C}{N}\int_0^T\left(1+\left|u'(t)\right|\right)dt\\&\le\frac{C}{N}\int_0^T\left(1+\frac{1}{\varepsilon}\exp\left(-\frac{\alpha t}{\varepsilon}\right)\right)dt\\&\le\frac{C}{N}\left(T+\frac{1}{\alpha}\left(1-\exp\left(-\frac{\alpha T}{\varepsilon}\right)\right)\right)\\&\le\frac{C}{N}.\end{aligned} \tag{3.20}$$

□

3.3. A posteriori error analysis

In this section, we shall derive an a posteriori error estimation for the numerical solution $\left\{u_i^N\right\}_{i=0}^N$. Recall that $\tilde{u}^N(t)$ is a piece-wise linear interpolation function through knots $\left(t_i,u_i^N\right),\ i=0,1,\cdots,N$. Then, for any $t\in J_i:=[t_{i-1},t_i]$, we obtain

$$\tilde{u}^N(t)=u_i^N+D^-u_i^N\left(t-t_i\right),\ i=1,2,\cdots,N. \tag{3.21}$$

Theorem 3.2. *Let $u(t)$ be the exact solution of problem (1.1), $\left\{u_i^N\right\}_{i=0}^N$ be the discrete solution of problem (3.4) and $\tilde{u}^N(t)$ be its piece-wise linear interpolation function defined in Eq (3.21). Then we have*

$$\left\|\tilde{u}^N(t)-u(t)\right\|_\infty\le C\max_{1\le i\le N}\left(h_i+h_i\left|D^-u_i^N\right|\right). \tag{3.22}$$

Proof. For any $t \in (t_{i-1}, t_i]$, it follows from Eq (1.1) and Eq (3.4) that

$$\begin{aligned} L\tilde{u}^N(t) - Lu(t) &= \varepsilon D^- u_i^N + f\left(t, \tilde{u}^N(t)\right) + \lambda \int_0^T K\left(t, s, \tilde{u}^N(s)\right) ds \\ &= -f\left(t_i, u_i^N\right) - \lambda \sum_{j=i}^{N} h_j K\left(t_i, t_j, u_j^N\right) \\ &\quad + f\left(t, \tilde{u}^N(t)\right) + \lambda \int_0^T K\left(t, s, \tilde{u}^N(s)\right) ds \\ &= P(t) + Q(t), \end{aligned} \tag{3.23}$$

where

$$P(t) = f\left(t, \tilde{u}^N(t)\right) - f\left(t_i, u_i^N\right), \tag{3.24}$$

$$Q(t) = \lambda \int_0^T K(t, s, \tilde{u}^N(s))\, ds - \lambda \sum_{j=1}^{N} h_j K\left(t_i, t_j, u_j^N\right). \tag{3.25}$$

With the assumptions of functions $f(t,u)$, $K(t,s,u)$ and the definition of $\tilde{u}^N(t)$, we have

$$\begin{aligned} |P(t)| &= \left| f\left(t_i, u_i^N\right) + \int_{t_i}^{t} \frac{df\left(\tau, \tilde{u}^N(\tau)\right)}{d\tau} d\tau - f\left(t_i, u_i^N\right) \right| \\ &\le \int_t^{t_i} \left(\left| \frac{\partial f\left(\tau, \tilde{u}^N\right)}{\partial \tau} \right| + \left| \frac{\partial f\left(\tau, \tilde{u}^N\right)}{\partial u} \right| \left| D^- u_i^N \right| \right) d\tau \\ &\le C h_i \left(1 + \left| D^- u_i^N \right|\right) \end{aligned} \tag{3.26}$$

and

$$\begin{aligned} |Q(t)| &= \left| \lambda \sum_{j=1}^{N} \int_{t_{j-1}}^{t_j} \left(K\left(t, s, \tilde{u}^N(s)\right) - K\left(t_i, t_j, u_j^N\right) \right) ds \right| \\ &\le |\lambda| \sum_{j=1}^{N} \int_{t_{j-1}}^{t_j} \left(\left| \frac{\partial}{\partial t} K\left(\xi_1 t + (1-\xi_1) t_i, s, \tilde{u}^N(s)\right)(t - t_i) \right| \right. \\ &\quad + \left| \frac{\partial}{\partial s} K\left(t_i, \xi_2 s + (1-\xi_2) t_j, \tilde{u}^N(s)\right)\left(s - t_j\right) \right| \\ &\quad \left. + \left| \frac{\partial}{\partial u} K\left(t_i, t_j, \xi_3 \tilde{u}^N(s) + (1-\xi_3) u_j^N\right)\left(\tilde{u}^N(s) - u_j^N\right) \right| \right) ds \\ &\le C \left(h_i + \max_{1 \le j \le N} h_j \left(1 + \left| D^- u_j^N \right|\right) \right), \end{aligned} \tag{3.27}$$

where $0 < \xi_1 < 1$, $0 < \xi_2 < 1$, and $0 < \xi_3 < 1$. The result can be derived from Eqs (3.23), (3.26), (3.27) and Corollary 2.1. □

From Corollary 3.1, it is easy to conclude that there exists a mesh $\{t_i\}_{i=0}^N$ and a monitor function $M(t)$ given in Eq (3.19) such that the inequality (3.17) holds true. However, $u'(t)$ is not available.

Therefore, based on the a posterior error estimation (3.22), we choose the discrete analogue of $M(t)$ as

$$\tilde{M}_i = 1 + \left|D^- u_i^N\right|, i = 1, 2, \cdots, N. \tag{3.28}$$

Therefore, the idea is to adaptively design a mesh in which the values of monitor function $tildeM_i$ are the same on each mesh interval. This is equivalent to find $\left\{\left(t_i, u_i^N\right)\right\}_{i=0}^N$, such that

$$h_i \tilde{M}_i = \frac{1}{N} \sum_{j=1}^{N} h_j \tilde{M}_j, \ i = 1, 2, \cdots, N. \tag{3.29}$$

Furthermore, to obtain this equidistributed mesh $\{t_i\}_{i=0}^N$ and the corresponding numerical solution u_i^N, we give the following iteration algorithm:

Algorithm 1 Steps of adaptive grid algorithm

1: **Step 1:** For a given N, let $\{t_i^{(0)}\}_{i=0}^N$ be an initial mesh with mesh step $\frac{1}{N}$. Choose a constant $\mu^* > 1$ that controls when the algorithm terminates.
2: **Step 2:** For a given mesh $\{t_i^{(k)}\}_{i=0}^N$ and numerical solution $\{u_i^{N,(k)}\}_{i=0}^N$, compute $\tilde{M}_i^{(k)}, i = 1, 2, \cdots, N$ in Eq (3.28) and set $\tilde{M}_0^{(k)} = 0$.
3: **Step 3:** Set $h_i^{(k)} = t_i^{(k)} - t_{i-1}^{(k)}$ for each i and set $L_0^{(k)} = 0$ and $L_i^{(k)} = \sum_{j=1}^{i} h_j^{(k)} \tilde{M}_j^{(k)}$ for $i = 1, 2, \cdots, N$. Define

$$\mu^{(k)} := \frac{N}{L_N^{(k)}} \max_{i=0,1,\cdots,N} h_i^{(k)} \tilde{M}_i^{(k)}. \tag{3.30}$$

4: **Step 4:** Set $Y_i^{(k)} = iL_N^{(k)}/N$ for $i = 0, 1, \cdots, N$. Interpolate (see [30, Remark 5.1]) to the points $(L_i^{(k)}, t_i^{(k)})$. Generate the new mesh $\{t_i^{(k+1)}\}_{i=0}^N$ by evaluating this interpolant at the $Y_i^{(k)}$ for $i = 0, 1, \cdots, N$.
5: **Step 5:** If $\mu^{(k)} \leq \mu^*$, then take $\{t_i^{(k+1)}\}_{i=0}^N$ as the final mesh and compute $\{u_i^{N,(k+1)}\}_{i=0}^N$. Otherwise return to Step 2.

4. Numerical experiments and discussion

In Section 4.1, We first present the iterative scheme. Then numerical experiments are given in Section 4.2 to validate the theoretical result of this paper. All experiments were performed on a Windows 10 (64 bit) PC-Intel(R) Core(TM) i5-4200H CPU 2.80 GHz, 8 GB of RAM using MATLAB R2021a.

4.1. Iterative scheme

In order to avoid solving the nonlinear equations (3.4), we apply the quasilinearization technique that performs a first-order Taylor expansion on the last iteration values and obtain

$$\begin{cases} u_i^{N,(k)} = \dfrac{\varepsilon/h_i u_{i-1}^{N,(k)} + B_i u_i^{N,(k-1)} + C_i}{\varepsilon/h_i + B_i}, i = 1, 2, \cdots, N, \\ u_0^{N,(k)} = A, \end{cases} \tag{4.1}$$

where

$$B_i = \frac{\partial}{\partial u} f\left(t_i, u_i^{N,(k-1)}\right), \tag{4.2}$$

$$C_i = -f\left(t_i, u_i^{N,(k-1)}\right) - \lambda \sum_{j=1}^{N} h_j K\left(t_i, t_j, u_j^{N,(k-1)}\right). \tag{4.3}$$

4.2. Numerical examples

For all the numerical experiments below, we choose $\mu^* = 1.1$, which is defined in Step 4 in Algorithm 1.

Example 4.1. *We consider a SPFIDE in the form [22]*

$$\begin{cases} \varepsilon u'(t) + 2u(t) + \tanh(u(t)) - e^t + \dfrac{1}{4}\displaystyle\int_0^1 t^2 \sin(u(s))\, ds = 0,\ t \in (0,1], \\ u(0) = 1. \end{cases} \tag{4.4}$$

Since the analytic solution of this problem is not available, we use the following formulas to calculate the errors and the corresponding convergence rates:

$$e_\varepsilon^N = \left\| \hat{\boldsymbol{u}}^{2N} - \boldsymbol{u}^N \right\|_\infty,\ p_\varepsilon^N = \log_2\left(\frac{e_\varepsilon^N}{e_\varepsilon^{2N}}\right), \tag{4.5}$$

where $\hat{\boldsymbol{u}}^{2N}$ is the numerical solution obtained on the fine mesh $\bar{\Omega}_{2N} = \bar{\Omega}_N \bigcup \left\{\frac{t_i + t_{i+1}}{2}\right\}_{i=0}^{N-1}$. The maximum errors and ε-uniform rates of the convergence are respectively defined as

$$e^N = \max_\varepsilon e_\varepsilon^N,\ p^N = \log_2\left(\frac{e^N}{e^{2N}}\right). \tag{4.6}$$

In the numerical experiments, we apply the presented adaptive grid algorithm to solve this problem. The resulting errors e_ε^N and the orders of the convergence p_ε^N, for particular values of ε and N are listed in Table 1. In addition, to compare the performance of the presented adaptive mesh with the Shishkin mesh [22] and the Bakhvalov mesh [23], some numerical results are given in Table 2.

According to the results in Table 1, for fixed N, the error increases with a diminishing speed and the convergence rate goes away from 1 as ε decreases , while for fixed ε, the error deceases to half as N doubles and the convergence rate is getting closer to 1. According to the results in Table 2, our adaptive mesh demonstrates both less error and more accurate first-order convergence rate than Shishkin mesh. In general, the performance of our adaptive grid algorithm is better when μ^* which is used to distribute the grid uniformly is closer to 1. However, the enhance becomes very limited after certain threshold and it can not work out successfully when μ^* is so close to 1 due to the enormous amount of calculations. Here the limitation of the adaptive mesh lies.

The behaviors of the numerical solution are presented in Figures 1, 2. Obviously, it can be seen that in these two figures the solution of the test problem decreases successively near to 0 at first and increases progressively close to 1 then and has a boundary layer at $t = 0$. Figure 3 shows the ε-uniform convergence of the method with different ε. To be more physical, the first-order uniform convergence

Table 1. The errors and corresponding convergence rates for Example 4.1.

ε	$N = 64$	$N = 128$	$N = 256$	$N = 512$	$N = 1024$
2^{-2}	0.004663	0.002384	0.001222	0.000619	0.000312
	0.9680	0.9637	0.9811	0.9903	-
2^{-4}	0.00595	0.003152	0.00163	0.000801	0.000412
	0.9167	0.9515	1.0244	0.9610	-
2^{-6}	0.006539	0.003482	0.001818	0.000939	0.000477
	0.9089	0.9373	0.9532	0.9769	-
2^{-8}	0.006711	0.003633	0.001893	0.000979	0.000501
	0.8853	0.9404	0.9514	0.9667	-
2^{-10}	0.006799	0.003635	0.001913	0.000996	0.000509
	0.9035	0.9258	0.9424	0.9667	-
2^{-12}	0.006881	0.003649	0.001926	0.000996	0.000512
	0.9151	0.9221	0.9505	0.9606	-
2^{-14}	0.006854	0.003683	0.001924	0.001	0.000513
	0.8963	0.9365	0.9447	0.9633	-
2^{-16}	0.00672	0.003752	0.001934	0.000999	0.000515
	0.8411	0.9562	0.9526	0.9560	-
e^N	0.006881	0.003752	0.001934	0.001	0.000515
p^N	0.8751	0.9562	0.9517	0.9569	-

Table 2. Comparisons of errors and corresponding convergence rates for Example 4.1.

N	$\varepsilon = 2^{-6}$			$\varepsilon = 2^{-8}$		
	Adaptive	Bakhvalov	Shishkin	Adaptive	Bakhvalov	Shishkin
3×2^5	4.53E-03	2.81E-03	7.18E-03	4.66E-03	2.83E-03	7.16E-03
	0.93	0.98	0.75	0.91	0.98	0.75
3×2^6	2.39E-03	1.42E-03	4.26E-03	2.48E-03	1.44E-03	4.25E-03
	0.94	0.99	0.79	0.95	0.99	0.79
3×2^7	1.24E-03	7.16E-04	2.46E-03	1.29E-03	7.23E-04	2.45E-03
	0.97	0.99	0.83	0.96	0.99	0.83
3×2^8	6.33E-04	3.59E-04	1.39E-03	6.62E-04	3.63E-04	1.38E-03
	0.98	1.00	0.85	0.97	1.00	0.85
3×2^9	3.20E-04	1.80E-04	7.71E-04	3.37E-04	1.82E-04	7.69E-04
	1.05	1.00	0.86	0.98	1.00	0.86
3×2^{10}	1.54E-04	9.01E-05	4.23E-04	1.71E-04	9.09E-05	4.22E-04

stands for our method in spite of violent changes of the numerical solution in the bound layer at $t = 0$. From Figure 3, no matter how close ε tends to zero, the maximum point-wise errors are bounded by $O\left(N^{-1}\right)$ which validates our theoretical analyses. For $\varepsilon = 2^{-8}$, Figure 4 displays how a mesh with $N = 64$ evolves through successive iterations of the algorithm by using monitor function (3.28).

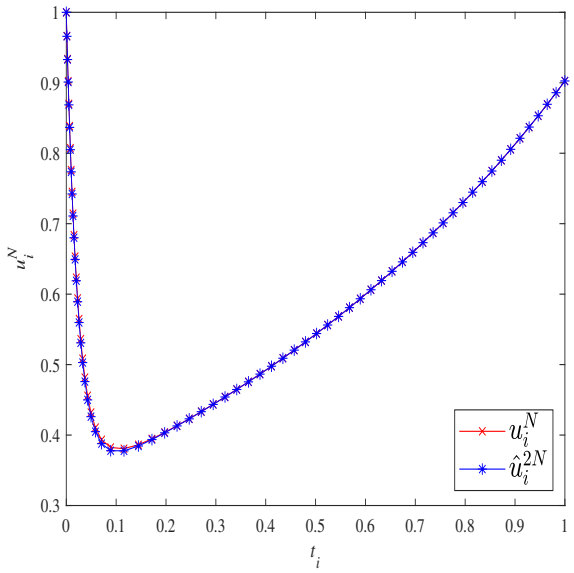

Figure 1. Numerical results of Example 4.1 for $N = 64$ and $\varepsilon = 2^{-4}$.

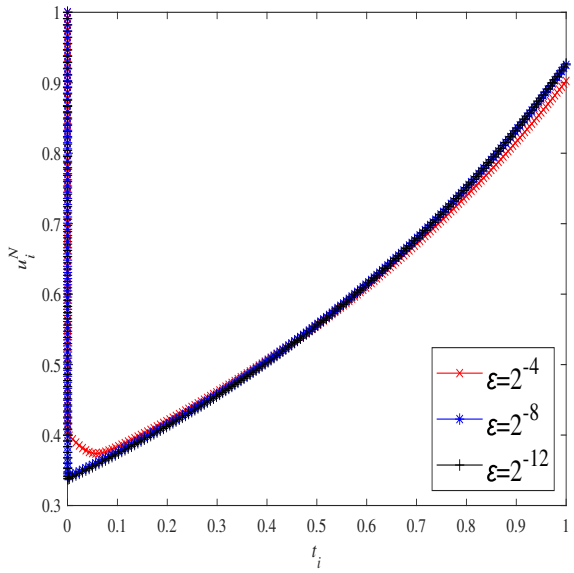

Figure 2. Numerical results of Example 4.1 for $N = 256$ and various ε.

Example 4.2. *We consider a first-order nonlinear singularly perturbed mixed type integro-differential equation in [24] in the form:*

$$\begin{cases} \varepsilon u'(t) + f(t, u(t)) + \dfrac{1}{2}\displaystyle\int_0^t u^2(s)ds + \dfrac{1}{2}\int_0^1 u^3(s)\,ds = 0,\ t \in (0, 1], \\ u(0) = 1. \end{cases} \tag{4.7}$$

where

$$f(t, u(t)) = \frac{\varepsilon}{4}u^2(t) + u(t) + \frac{\varepsilon}{6}e^{-\frac{3}{\varepsilon}} - \frac{5}{12}\varepsilon. \tag{4.8}$$

It is testified that it satisfies the assumption (3.10). The analytic solution of this problem is $u(t) = e^{-t/\varepsilon}$. We use the following formulas to calculate the errors and the corresponding convergence rates:

$$e_\varepsilon^N = \max_{0\le i\le N}\left|u_i^N - u_i\right|,\ p_\varepsilon^N = \log_2\left(\frac{e_\varepsilon^N}{e_\varepsilon^{2N}}\right). \tag{4.9}$$

The maximum errors and ε-uniform convergence rates are defined in Eq (4.6).

The resulting errors e_ε^N and the orders of the convergence p_ε^N, for particular values of ε and N are listed in Table 3. In addition, to compare the performance of the presented adaptive mesh with the Shishkin mesh [22] and the Bakhvalov mesh [23], some numerical results are given in Table 4.

Table 3. The errors and corresponding convergence rates for Example 4.2.

ε	$N = 64$	$N = 128$	$N = 256$	$N = 512$	$N = 1024$
2^{-2}	0.008698	0.004386	0.002202	0.001103	0.000552
	0.9880	0.9939	0.9969	0.9985	-
2^{-4}	0.011073	0.00562	0.002799	0.001413	0.00071
	0.9783	1.0057	0.9863	0.9929	-
2^{-6}	0.012473	0.00639	0.003247	0.001638	0.0008
	0.9648	0.9767	0.9876	1.0335	-
2^{-8}	0.013236	0.006774	0.003463	0.00176	0.000887
	0.9664	0.9681	0.9763	0.9881	-
2^{-10}	0.013376	0.006909	0.003559	0.00181	0.000917
	0.9530	0.9570	0.9755	0.9814	-
2^{-12}	0.013461	0.006954	0.003575	0.001835	0.000929
	0.9528	0.9601	0.9619	0.9822	-
2^{-14}	0.013563	0.007002	0.003592	0.001836	0.000937
	0.9540	0.9631	0.9680	0.9704	-
2^{-16}	0.015521	0.007146	0.003596	0.001842	0.000935
	1.1190	0.9908	0.9647	0.9784	-
e^N	0.015521	0.007146	0.003596	0.001842	0.000937
p^N	1.1190	0.9908	0.9647	0.9755	-

Table 4. Comparisons of errors and corresponding convergence rates for Example 4.2.

N	$\varepsilon = 2^{-6}$			$\varepsilon = 2^{-8}$		
	Adaptive	Bakhvalov	Shishkin	Adaptive	Bakhvalov	Shishkin
3×2^5	8.43E-03	2.15E-02	1.91E-02	8.95E-03	2.69E-02	1.67E-02
	0.97	0.90	1.28	0.97	0.65	0.11
3×2^6	4.31E-03	1.15E-02	7.85E-03	4.58E-03	1.72E-02	1.54E-02
	0.98	0.94	1.29	0.97	0.67	0.80
3×2^7	2.18E-03	6.00E-03	3.21E-03	2.33E-03	1.08E-02	8.88E-03
	1.04	0.97	1.00	0.98	0.90	1.28
3×2^8	1.06E-03	3.06E-03	1.61E-03	1.18E-03	5.78E-03	3.65E-03
	0.97	0.98	0.85	0.99	0.93	1.32
3×2^9	5.39E-04	1.55E-03	8.88E-04	5.93E-04	3.02E-03	1.46E-03
	0.98	0.99	0.87	1.00	0.97	1.41
3×2^{10}	2.72E-04	7.78E-04	4.87E-04	2.98E-04	1.54E-03	5.51E-04

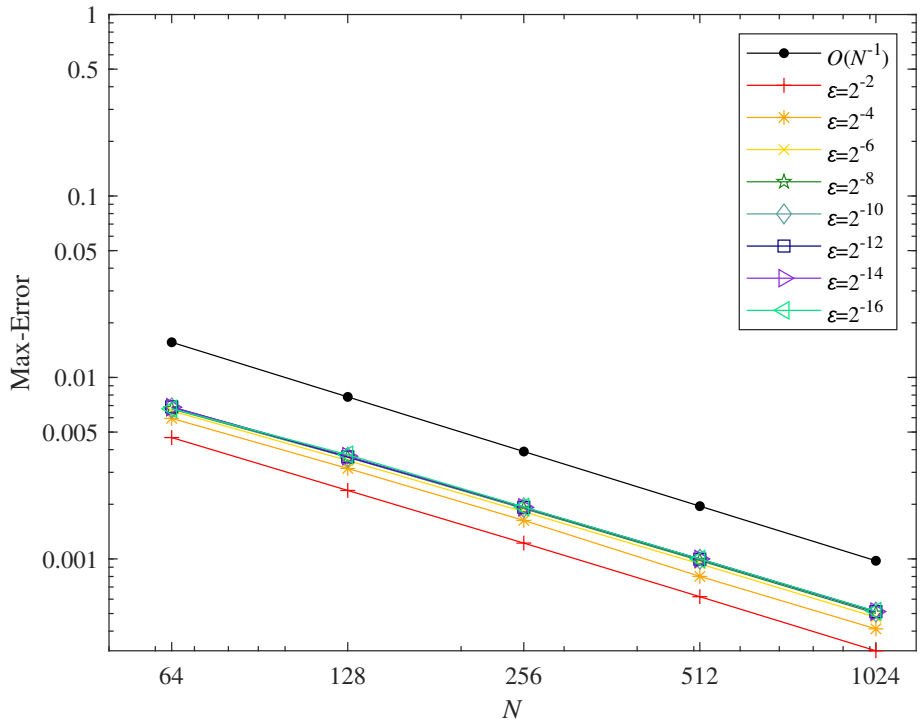

Figure 3. Maximum point-wise errors of log-log plot for Example 4.1.

The behaviors of the numerical solution are presented in Figures 5, 6. Obviously, it can be seen that in these two figures the solution of the test problem gradually decreases to zero with a decreasing velocity rate as well as has a boundary layer at $t = 0$. Figure 7 shows the ε-uniform convergence of the method with different ε. From Figure 7, no matter how close ε tends to zero, the maximum point-wise errors are bounded by $O\left(N^{-1}\right)$ which validates our theoretical analyses. For $\varepsilon = 2^{-8}$, Figure 8 displays how a mesh with $N = 64$ evolves through successive iterations of the algorithm by using monitor function (3.28).

The unique but significant difference between these two examples can be found in Table 4. At the situation $\varepsilon = 2^{-8}$, adaptive mesh demonstrates better than Bakhvalov mesh. This is because the construction of the Bakhvalov mesh is based on prior information of the exact solution. Therefore the effect of this method is tightly relevant to the form of equation. The existing Bakhvalov mesh may display wonderful at suitable equations but poor when it is adverse. However, the adaptive mesh based on posterior error estimate requires none of prior information of the exact solution and displays steadily at various equations.

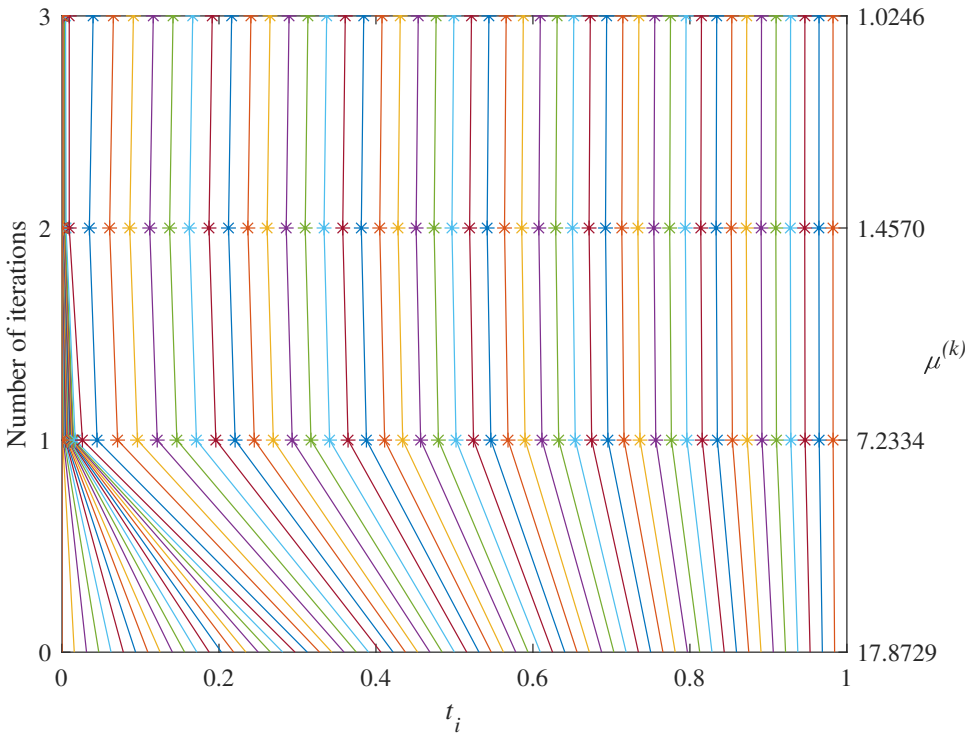

Figure 4. Evolution of the mesh for Example 4.1.

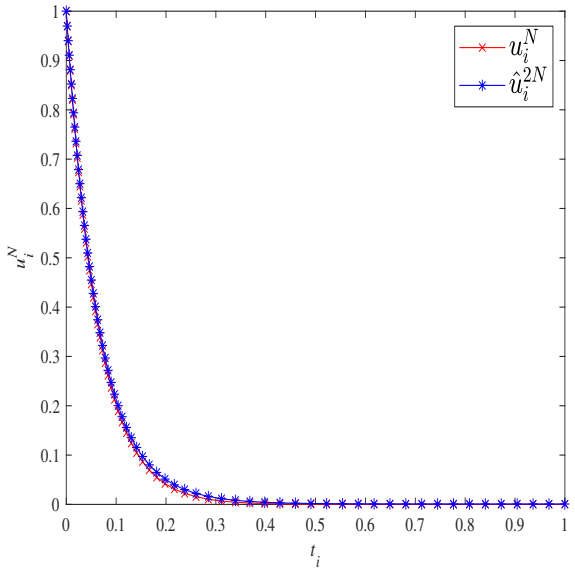

Figure 5. Numerical results of Example 4.2 for $N = 64$ and $\varepsilon = 2^{-4}$.

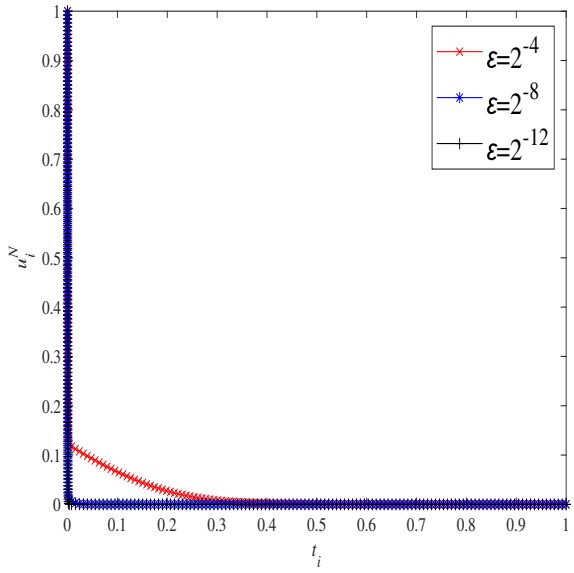

Figure 6. Numerical results of Example 4.2 for $N = 256$ and various ε.

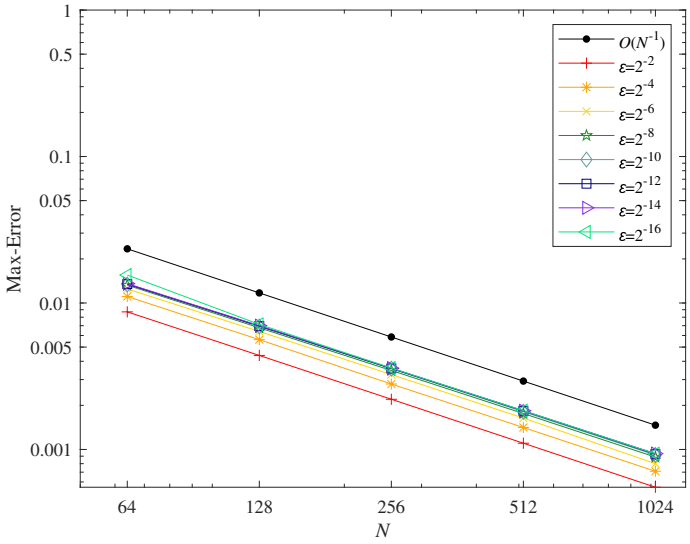

Figure 7. Maximum point-wise errors of log-log plot for Example 4.2.

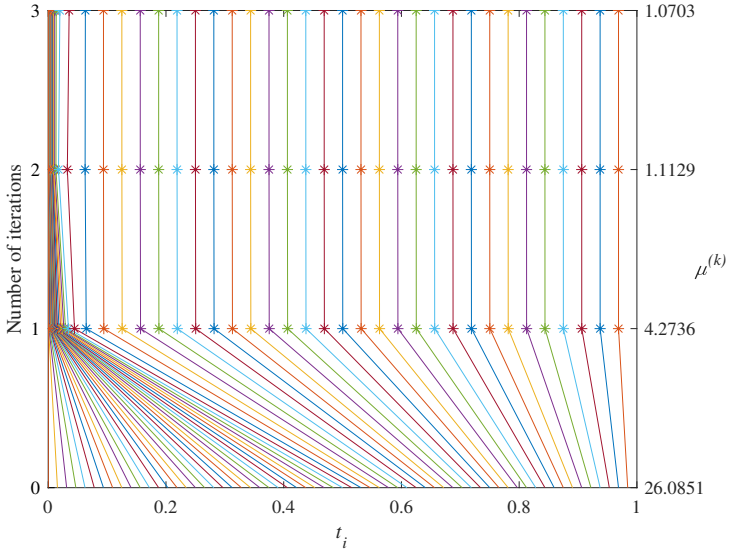

Figure 8. Evolution of the mesh for Example 4.2.

5. Concluding remarks

This paper considers a nonlinear singularly perturbed Fredholm integro-differential equation for a first-order initial value problem. A first-order ε-uniformly convergent numerical method for solving this problem is presented, which comprises an adaptive grid based on the posterior error estimate and the mesh equidistribution principle. The difference scheme including the weights and the remainders is established using the backward Euler formula for the derivative term, together with the composite right rectangle quadrature rule for the integral term. A theoretical analysis based on prior error bound is conducted to prove the first-order convergence of the proposed method. Two examples show that our adaptive mesh demonstrates better than Shishkin mesh and performs as well as Bakhvalov mesh. In the future, we will try to extend the proposed adaptive grid method for solving other related integro-differential equations which can be found in [5, 6, 31].

Conflict of interest

The authors declare there is no conflict of interest.

References

1. D. O'Regan, M. Meehan, *Existence theory for nonlinear integral and integrodifferential equations. mathematics and its applications,* Springer, Dordrecht, (1998), 14–36. https://doi.org/10.1007/978-94-011-4992-1
2. K. Alexander, P. Lukas, Modeling infectious diseases using integro-differential equations: optimal control strategies for policy decisions and applications in COVID-19, *Researchgate*, preprint (2022). https://doi.org/10.13140/RG.2.2.10845.44000
3. Z. Guo, Z. T. Guo, L. Y. Yi, Analysis of multicrack problems with eigen COD boundary integral equations, *Appl. Math. Mech.* (in Chinese), **40** (2019), 200–209. https://doi.org/10.21656/1000-0887.390183
4. L. Prandtl, Motion of fluids with very little viscosity, 1928. Available from: https://ntrs.nasa.gov/citations/19930090813
5. Y. L. Zhao, X. M. Gu, A. Ostermann, A preconditioning technique for an all-at-once system from Volterra subdiffusion equations with graded time steps, *J. Sci. Comput.*, **88** (2021). https://doi.org/10.1007/s10915-021-01527-7
6. X. M. Gu, S. L. Wu, A parallel-in-time iterative algorithm for Volterra partial integro-differential problems with weakly singular kernel, *J. Comput. Phys.*, **417** (2022), 109576. https://doi.org/10.1016/j.jcp.2020.109576
7. H. Badawi, N. Shawagfeh, O. A. Arqub, Fractional conformable stochastic integrodifferential equations: existence, uniqueness, and numerical simulations utilizing the shifted Legendre spectral collocation algorithm, *Math. Probl. Eng.*, (2022). https://doi.org/10.1155/2022/5104350
8. H. Badawi, O. A. Arqub, N. Shawagfeh, Well-posedness and numerical simulations employing Legendre-shifted spectral approach for Caputo–Fabrizio fractional stochastic integrodifferential equations, *Int. J. Mod. Phys. C*, (2023). https://doi.org/10.1142/S0129183123500705

9. H. Sweis, O. A. Arqub, N. Shawagfeh, Fractional delay integrodifferential equations of nonsingular kernels: existence, uniqueness, and numerical solutions using Galerkin algorithm based on shifted Legendre polynomials, *Int. J. Mod. Phys. C*, (2023). https://doi.org/10.1142/S0129183123500523

10. M. A. Aal, S. Djennadi, O. A. Arqub, H. Alsulami On the recovery of a conformable time-dependent inverse coefficient problem for diffusion equation of periodic constraints type and integral over-posed data *Math. Probl. Eng.*, (2022). https://doi.org/10.1155/2022/5104725

11. M. Mandal, A. Kayal, G. Nelakanti, Projection methods for approximate solution of a class of nonlinear Fredholm integro-differential equations, *Appl. Numer. Math.*, **184** (2023), 49–76. https://doi.org/10.1016/j.apnum.2022.09.019

12. J. Chen, M. He, Y. Huang, A fast multiscale Galerkin method for solving second order linear Fredholm integro-differential equation with Dirichlet boundary conditions, *J. Comput. Appl. Math.*, **364** (2020), 112352. https://doi.org/10.1016/j.cam.2019.112352

13. J. Huang, Z. Cen, A. Xu, L. B. Liu, A posteriori error estimation for a singularly perturbed Volterra integro-differential equation, *Numer. Algor.*, **83** (2020), 549–563. https://doi.org/10.1007/s11075-019-00693-y

14. S. Kumar, J. Vigo-Aguiar, Analysis of a nonlinear singularly perturbed Volterra integro-differential equation, *J. Comput. Appl. Math.*, **404** (2021), 113410. https://doi.org/10.1016/j.cam.2021.113410

15. L. B. Liu, Y. P. Chen, Y. Liang, Numerical analysis of a nonlinear singularly perturbed delay Volterra integro-differential equation on an adaptive grid, *J. Comp. Math.*, **40** (2022), 258–274. https://doi.org/10.4208/jcm.2008-m2020-0063

16. Y. Liang, L. B. Liu, Z. D. Cen, A posteriori error estimation in maximum norm for a system of singularly perturbed Volterra integro-differential equations, *Comp. Appl. Math.*, **39** (2020), 255. https://doi.org/10.1007/s40314-020-01303-7

17. E. Cimen, M. Cakir, A uniform numerical method for solving singularly perturbed Fredholm integro-differential problem, *Comput. Appl. Math.*, **40** (2021), 42. https://doi.org/10.1007/s40314-021-01412-x

18. G. M. Amiraliyev, M. E. Durmaz, M. Kudu, A numerical method for a second order singularly perturbed Fredholm integro-differential equation, *Miskolc Math. Notes*, **22** (2021), 37–48. https://doi.org/10.18514/MMN.2021.2930

19. M. E. Durmaz, M. Cakir, I. Amirali, G. M. Amiraliyev, Numerical solution of singularly perturbed Fredholm integro-differential equations by homogeneous second order difference method, *J. Comput. Appl. Math.*, **412** (2022), 114327. https://doi.org/10.1016/j.cam.2022.114327

20. M. E. Durmaz, I. Amirali, G. M. Amiraliyev, An efficient numerical method for a singularly perturbed Fredholm integro-differential equation with integral boundary condition, *J. Appl. Math. Comput.*, preprint (2022). https://doi.org/10.1007/s12190-022-01757-4

21. D. Kumar, K. Deswal, S. Singh, Wavelet-based approximation with non-standard finite difference scheme for singularly perturbed partial integro-differential equation, *Comp. Appl. Math.*, **41** (2022), 341. https://doi.org/10.1007/s40314-022-02053-4

22. M. Cakir, Y. Ekinci, E. Cimen, A numerical approach for solving nonlinear Fredholm integro-differential equation with boundary layer, *Comp. Appl. Math.*, **41** (2022), 259. https://doi.org/10.1007/s40314-022-01933-z

23. M. Brdar, H. Zarin, A singularly perturbed problem with two parameters on a Bakhvalov-type mesh, *J. Comput. Appl. Math.*, **292** (2016), 307–319. https://doi.org/10.1016/j.cam.2015.07.011

24. M. Cakir, B. Gunes, Exponentially fitted difference scheme for singularly perturbed mixed integro-differential equations, *Georgian Math. J.*, **29** (2022), 193–203. https://doi.org/10.1515/gmj-2021-2130

25. N. Kopteva, Maximum norm a posteriori error estimates for a one-dimensional convection-diffusion problem, *SIAM J. Numer. Anal. S*, **39** (2001), 423–441. https://epubs.siam.org/doi/10.1137/S0036142900368642

26. N. Kopteva, M. Stynes, A robust adaptive method for a quasi-linear one-dimensional convection-diffusion problem, *SIAM J. Numer. Anal. S*, **39** (2001), 1446–1467. https://epubs.siam.org/doi/10.1137/S003614290138471X

27. Z. Mao, L. B. Liu, A moving grid algorithm for a strongly coupled system of singularly perturbed convection-diffusion problems, *Math. Appl. (Wuhan)*, **31** (2018), 653–660. https://10.13642/j.cnki.42-1184/o1.2018.03.048

28. L. B. Liu, C. W. Zhu, G. Q. Long, Numerical analysis of a system of semilinear singularly perturbed first-order differential equations on an adaptive grid, *Math. Methods Appl. Sci.*, **45** (2022), 2042–2057. https://doi.org/10.1002/mma.7904

29. Y. Qiu, D. M. Sloan, T. Tang, Numerical solution of a singularly perturbed two point boundary value problem using equidistribution: analysis of convergence, *J. Comput. Appl. Math.*, **116** (2000), 121–143. https://doi.org/10.1016/S0377-0427(99)00315-5

30. N. Kopteva, N. Madden, M. Stynes, Grid equidistribution for reaction–diffusion problems in one dimension, *Numer. Algorithms*, **40** (2005), 305–322. https://doi.org/10.1007/s11075-005-7079-6

31. X. M. Gu, H. W. Sun, Y. L. Zhao, X. Zheng, An implicit difference scheme for time-fractional diffusion equations with a time-invariant type variable order, *Appl. Math. Lett.*, **120** (2021), 107270. https://doi.org/10.1016/j.aml.2021.107270

AIMS Press